Draft version 1.0

CEPC NOTE

CEPC_ANA_HIG_2015_XXX

April 26, 2017

Measurement of the branching ratio BR($H \to WW^*$) at CEPC

LIAO Libo[a,b], LI Gang[b], RUAN Manqi[b], LI Kang[a], and XU Qingjun[a]

[a]Hangzhou Normal University
[b]Institute of High Energy Physics

Abstract

It's a note for $e^+e^- \to ZH, Z \to ee, H \to WW^*$ channel analysis.

- **Title:** Branch ratio measurement of $H \to WW^*$ at CEPC.
- **Author list:** it will be provided by the CEPC Collaboration, and will be made available on their website. On the front page, you should name "The CEPC Collaboration" as author.
- **Abstract:** Based on a Monte Carlo sample with planed lumonisity of $5ab^{-1}$ at CEPC, measurement of H to WW^* has been performed under full simulation. In this analysis, two decay modes of WW^*, which are $WW^* \to l^+l^-\nu\bar{\nu}$ and $WW^* \to l\nu jj$, are studied.

E-mail address: liaolb@ihep.ac.cn

Contents

1 Introduction

The precise measurement of the Higgs boson properties has become a high priority target for the particle physics community worldwide 5 years after the particle discovery [1]. In order to carry out this programme at the required precision, dedicated Higgs factories are needed. The LHC is an excellent Higgs factory, which led to the Higgs boson discovery and its first property measurements. Despite its success, the LHC is limited by enormous backgrounds and large theoretical and systematic uncertainties, which limit the precision of the Higgs boson measurements to the level of 5-10%. This precision is not adequate to differentiate between the SM and various new physics models [citation needed].

On the other hand, an electron positron collider provides a unique physics opportunity to improve the precision of the Higgs boson property measurements beyond the reach of the LHC. It can measure the absolute values of the Higgs boson couplings, the Higgs boson width, and, in addition, it has unique sensitivity to Higgs boson exotic decay modes. Besides, the e^+e^- collider physics programme is complementary to that of proton colliders. All these have stimulated the interest of the particle physics community worldwide and various different e^+e^- facilities have been proposed.

The CEPC is a circular e^+e^- collider with a total circumference of 50 - 100km. It is expected to deliver one million Higgs bosons, which will be detected and reconstructed with almost 100% efficiency during 10 years operation and with 2 detectors. Such a sample will allow the measurement of Higgs boson couplings with precision of 0.1–1% level, which is one order of magnitude better than the current HL-LHC expectation [citation needed].

At the CEPC with center-mass of energy $\sqrt{s}$ = 250 GeV and non-polarized beams, Higgs bosons are produced through Higgsstrahlung, which dominates, and vector boson fusion, see Figure 1.

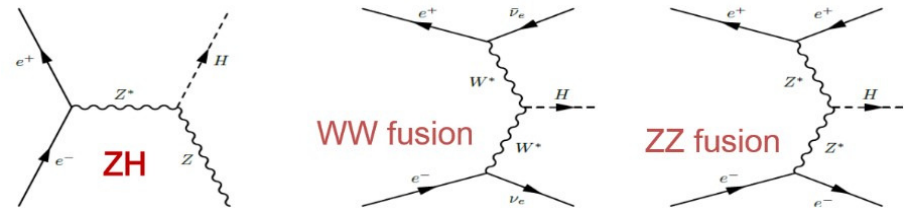

Figure 1: Feynman diagrams for Higgs boson production mechanisms at CEPC

1.1 Classification of signal final states

A full simulation study of the measurement of Br($H \to WW^*$) at the CEPC is highly motivated. First of all, the SM Higgs boson branching ratio to WW is 22%, which renders is the most important channel to study the HWW coupling at the CEPC. Moreover, the Br($H \to WW^*$) measurement is also a key ingredient for the determination of the Higgs boson width. Last but not least, the W bosons decay into various physics objects (leptons, missing energy and momentum, taus and jets), providing an excellent benchmark to evaluate detector performance. The current status of the CEPC full simulation studies for the measurement of Br($H \to WW^*$) is reported in this manuscript.

For the studies discussed here, the $H \to WW^*$ decays are classified into 50 different channels according to the number of electrons, muons, tau-leptons, neutrinos and jets in the final state. Assuming one million Higgs bosons, the expected yield for $H \to WW^*$ events in these final states is presented in Table 1. These final states are further classified into four categories depending on the number of jets in the event. As shown in Table 1 there can be, zero, two, four or six jet events.

W boson decay \ Z boson decay	ee	$\mu\mu$	$\tau\tau$	$\nu\nu$	qq
$WW^* \to e\nu e\nu$	95	89	89	612	1791
$WW^* \to \mu\nu\mu\nu$	94	87	87	601	1758
$WW^* \to e\nu\mu\nu$	188	176	176	1212	3548
$WW^* \to e\nu\tau\nu$	201	188	187	1292	3783
$WW^* \to \mu\nu\tau\nu$	109	186	186	1280	3747
$WW^* \to \tau\nu\tau\nu$	156	99	99	683	1998
$WW^* \to e\nu qq$	1195	1117	1115	7704	22560
$WW^* \to \mu\nu qq$	1184	1106	1104	7632	22349
$WW^* \to \tau\nu qq$	1263	1180	1177	8136	23825
$WW^* \to qqqq$	3764	3518	3510	24264	71051

Table 1: Signal events passing the $Z \to X, H \to WW^*, WW^* \to X$ selection criteria [which?]. The different colours denote different jet categories: zero-jet category (gray), two-jet category (green), four-jet category (magenta), and six-jet category (red).

In this note, a representative analysis of each jet category is reported in detail. For the zero-jet category, $e^+e^- \to ZH, Z \to \mu^+\mu^-, H \to WW^*, WW^* \to e\nu\mu\nu$ decay chain has been considered. For categories with jets the following decay chains have been studied: $e^+e^- \to ZH, Z \to e^+e^-, H \to WW^*, WW^* \to \mu\nu qq$ (two-jet category) and $e^+e^- \to ZH, Z \to \nu\nu, H \to WW^*, WW^* \to qqqq$ (four-jet category). The six-jet category is more complicated and will be the topic of a future analysis.

2 MC samples

2.1 Simulation and analysis tools

This analysis is performed using simulated data that correspond to an integrated luminosity of 5000fb^{-1} at $\sqrt{s} = 250$ GeV. The cross section for the various processes relevant for this energy is shown in Figure 2. For all signal samples a Higgs boson mass of $m_H = 125$ GeV is assumed. Background events are generated by Whizard 1.95 and include ISR. The detector model, cepc_v1, is simulated by `Geant4`. Object reconstruction is done using the particle-flow algorithm, `Arbor`. Charged particle identification is performed by LICH, which is a TMVA-based [citation needed] software package optimized for a high granularity calorimeter. The ee-k_T clustering algorithm is used for jet clustering and the performance of the b-tagging algorithm is given by LCFIPlus package.

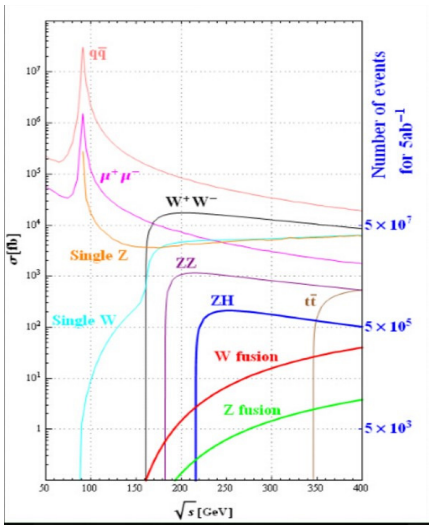

(a)

	240GeV	250GeV
qq	54662	50216
$\mu^+\mu^-$	4685	4405
single Z	4538	4734
single W	5086	5144
W^+W^-	16004	15484
ZZ	1079	1033
ZH	203	212
W fusion	5.36	6.72
Z fusion	0.50	0.63

(b)

Figure 2: 2(a): The distribution of cross section of the Standard Model when center mass of system is near 250 GeV. 2(b): The specific value of cross section of the main Standard Model when center mass of system is 240 GeV and 250 GeV

The SM backgrounds included in this search are classified in two-fermion and four-fermion final states. Two fermion backgrounds include Bhabha scattering and the production of $\mu^+\mu^-$, $\tau^+\tau^-$, $\nu\bar{\nu}$ and $q\bar{q}$ pairs. Four fermion background consist of rest of the Standard Model backgrounds. This includes also ZH production in which the Higgs boson decays to channels other than WW.

2.2 Pre-selection

The total background to the branching ratio measurement amounts to more than 70 million events. Many of those events, however, have completely different topologies compared to signal, and therefore the decision to reject them can be made at an early stage, even before the simulation.

The events are categorized to four classes: $llH(l = e, \mu)$, $\tau\tau H$, $\nu\nu H$ and qqH. Subsequently, a loose selection is performed on the objects before they are passed to the full detector simulation, which will be referred to in the following as pre-selection. The pre-selection is such that it is fully efficient for signal events.

2.2.1 Pre-selection of $e^+e^- \to ZH, Z \to l^+l^-(l = e, \mu), H \to X$ decay

Compared to the Standard Model background, the most distinguishing feature of $Z \to l^+l^-(l = e, \mu), H \to X$ decays is the invariant mass and the recoil mass of Z boson. For the pre-selection, a di-lepton pair compatible with the Z boson is identified [how?] and subsequently a window in the di-lepton invariant mass and in the recoil mass is required with numerical values shown in Table 2.

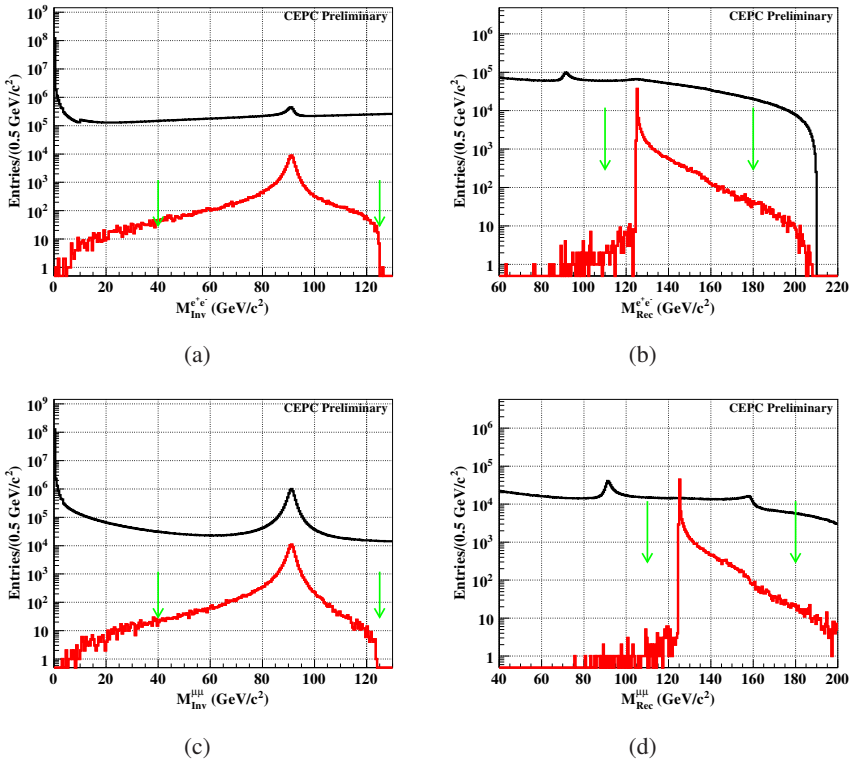

Figure 3: The distribution of invariant mass and recoil mass of the best candidate of Z boson. Red line is the distribution of Higgs signal. Black line is the distribution of the Standard Model background. TOP: These two plots are the mass distribution of $Z \to e^+e^-, H \to X$ decay. Bottom: The left is invariant mass distribution and right is recoil mass distribution of $Z \to \mu^+\mu^-, H \to X$ decay

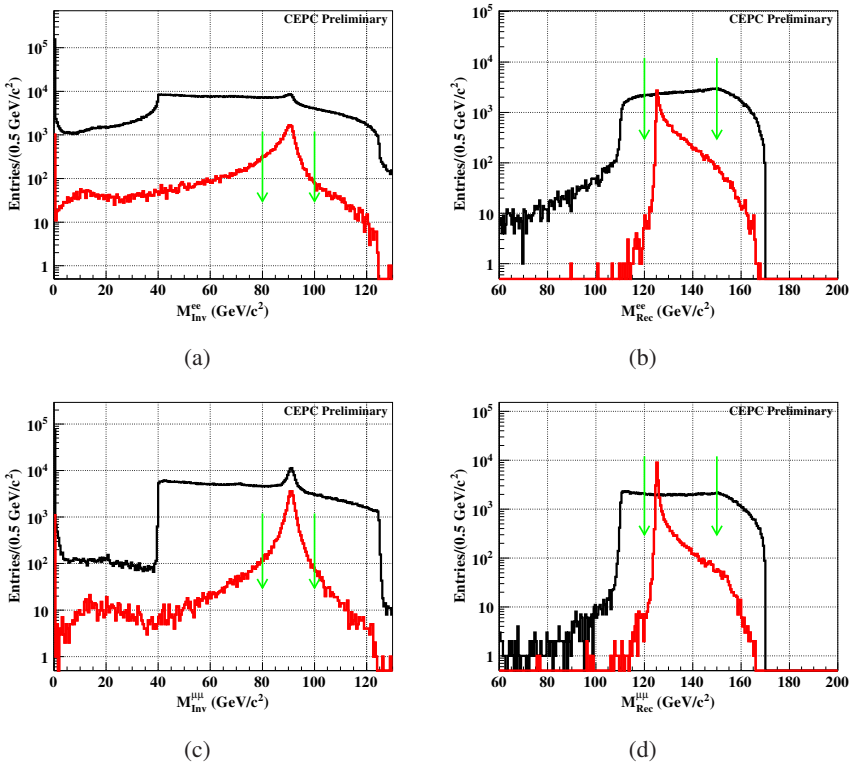

Figure 4: The distribution of invariant mass and recoil mass of the best candidate of Z boson in full simulation. Red line is the distribution of Higgs signal. Black line is the distribution of the Standard Model background. TOP: These two plots are the mass distribution of $Z \to e^+e^-, H \to X$ decay. Bottom: The left is invariant mass distribution and right is recoil mass distribution of $Z \to \mu^+\mu^-, H \to X$ decay

Process of signal	eeH process	$\mu\mu H$ process
conditions of pre-selection	$40\ \mathrm{GeV}/c^2 < M^{ee}_{Inv} < 130\ \mathrm{GeV}/c^2$ $110\ \mathrm{GeV}/c^2 < M^{ee}_{Rec} < 180\ \mathrm{GeV}/c^2$	$40\ \mathrm{GeV}/c^2 < M^{\mu\mu}_{Inv} < 130\ \mathrm{GeV}/c^2$ $110\ \mathrm{GeV}/c^2 < M^{\mu\mu}_{Rec} < 180\ \mathrm{GeV}/c^2$
conditions of validation	$80\ \mathrm{GeV}/c^2 < M^{ee}_{Inv} < 100\ \mathrm{GeV}/c^2$ $120\ \mathrm{GeV}/c^2 < M^{ee}_{Rec} < 150\ \mathrm{GeV}/c^2$	$80\ \mathrm{GeV}/c^2 < M^{\mu\mu}_{Inv} < 100\ \mathrm{GeV}/c^2$ $120\ \mathrm{GeV}/c^2 < M^{\mu\mu}_{Rec} < 150\ \mathrm{GeV}/c^2$

Table 2: Conditions of pre-selection in MC and validation in full simulation. Considered the resolution of detector, the conditions of validation should be more strict.

This pre-selection is highly efficient for signal (more than 95% of signal event are retained), whereas at the same time more than 99% of the background events are rejected. It has also been verified that there is no bias after pre-selection [how???].

2.2.2 Pre-selection of $e^+e^- \to ZH, Z \to \nu\bar{\nu}, H \to X$ decay.

The pre-selection definition for $\nu\nu H$ channel is more difficult to choose compared to eeH and $\mu\mu H$ decay chains. Due to the $Z \to \nu\nu$ decay, it is possible to use the missing mas of the system to discriminate between signal and background. In addition to the missing mass, the total mass and the total transverse momentum are used, as well as the constraint $|cos\theta| > 0.99$ [what is this angle?].

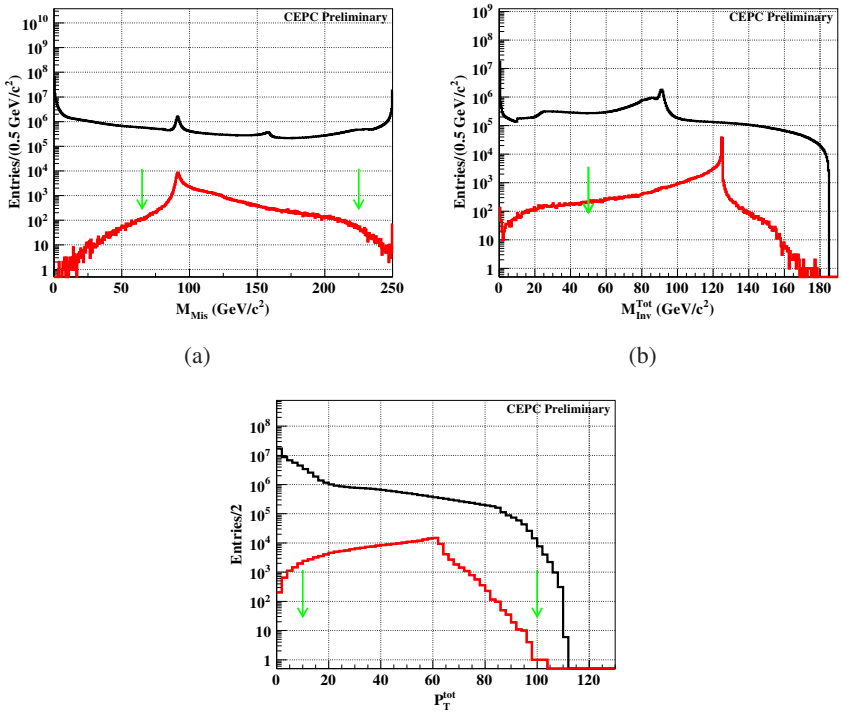

(a) (b)

(c)

Figure 5: The distribution of missing mass, total mass and total transverse momentum in MC truth. Red line is the distribution of Higgs signal. Black line is the distribution of the Standard Model background. Top: The left is missing mass of system. The right is total mass of system. Bottom: It is the distribution of total transverse momentum of system, and the peak of background is caused by angle constraint of two fermion background.

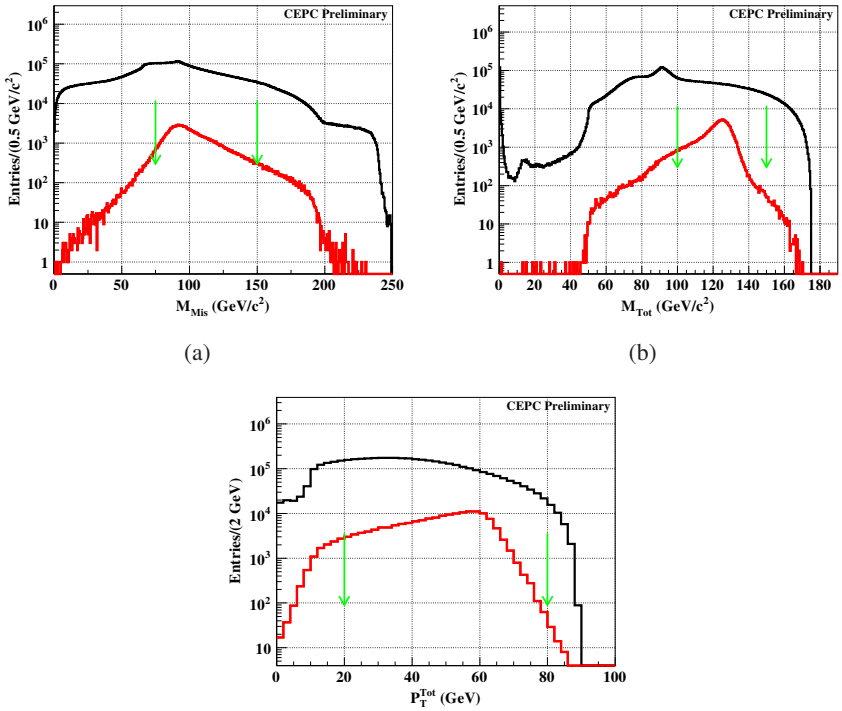

Figure 6: The distribution of missing mass, total mass and total transverse momentum in full simulation. Red line is the distribution of Higgs signal. Black line is the distribution of the Standard Model background. Top: The left is missing mass of system. The right is total mass of system. Bottom: It is the distribution of total transverse momentum of system.

Process of signal	$\nu\nu H$
conditions of pre-selection	$65\ \mathrm{GeV}/c^2 < M_{Mis} < 225\ \mathrm{GeV}/c^2$ $M_{Tot} > 50\ \mathrm{GeV}/c^2$ $10\ \mathrm{GeV}/c < p_T < 100\ \mathrm{GeV}/c$
conditions of validation	$75\ \mathrm{GeV}/c^2 < M_{Mis} < 150\ \mathrm{GeV}/c^2$ $100\ \mathrm{GeV}/c^2 < M_{Tot} < 150\ \mathrm{GeV}/c^2$ $20\ \mathrm{GeV}/c < p_T < 80\ \mathrm{GeV}/c$

Table 3: Conditions of pre-selection in MC and validation in full simulation of $\nu\nu H$ process

As shown in Figure 5, the distributions of signal and background are similar, so we should be careful to do filter to reject bias, and we choose the conditions as shown in Table 3. Percent of each channel has changed after pre-selection, but it makes sense for analysis.

After reconstructed, we can get distribution of the same variables, as shown in Figure 6. Considering the resolution of detector in full simulation, the conditions of validation should be more strict.

3 Measurement of $Br(H \to WW^*)$

After pre-selection, the fundamental for measurement of branch ratio is complete. As mentioned previously, due to the large number of possible decay chains, only a subset of them will be considered in the following.

3.1 Analysis of $e^+e^- \to ZH, Z \to \mu^+\mu^-, H \to WW^*, WW^* \to e\nu\mu\nu$ decay

3.1.1 Event selection

It is a chosen channel because only two visible particles in final states from W bosons. Therefore, the background would be suppressed effectively by different lepton flavors. And only leptonic decay of b-jets, W boson and τ would be survived.

Referred to the Moxin's article **??**, only few number of $ZZ \to \mu^+\mu^-\tau^+\tau^-$ decay and $ZZ \to 4\tau$ decay would not be rejected by requiring three muons and one electron and number of remain particles are less than 3. So the Higgs background would be main background compared to the Standard Model background.

Furthermore, the spatial resolution of vertex detector(VTX) of CEPC constructed with high resolution pixel sensors near the interacted point(IP) is better than 3 μm, so leptonic decay of τ and b-jet would be rejected effectively by a constructed function, which is $\sqrt{(\frac{D_0}{sigD_0})^2 + (\frac{Z_0}{sigZ_0})^2} < 5$.

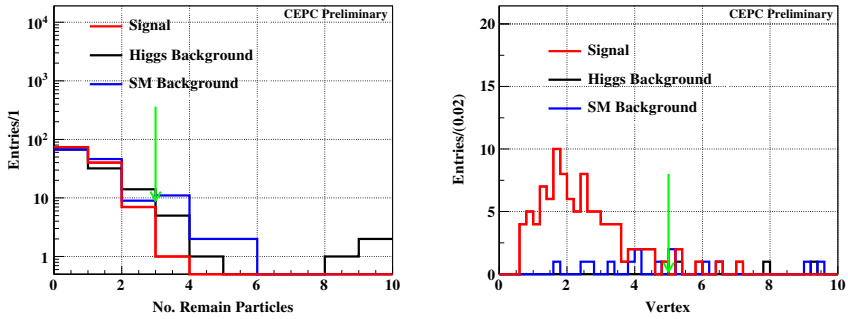

(a) (b)

Figure 7: 7(a) The No. remain particles of $e^+e^- \to ZH, Z \to \mu^+\mu^-, H \to WW^*, WW^* \to e\nu\mu\nu$ decay. Except for four tracks, there are few photons, so we can veto semi-leptonic decay and hadronic decay of background. 7(b) The distribution of Vertex of $e^+e^- \to ZH, Z \to \mu^+\mu^-, H \to WW^*, WW^* \to e\nu\mu\nu$ decay. And there are two leptons totally from W boson, so we plus the value of each lepton. And leptons from τ and b-jet would fly a long distance, so they would be rejected effectively.

After event selection in, final number of events of signal and background are in Table 4. And the main background of this channel is $e^+e^- \to ZZ \to \tau^+\tau^-\mu^+\mu^-$, as shown in Table 5.

Category	Signal	ZH background	SM background
Total	172	34624	700311
Validation of pre-selection	136	29263	117395
$N_{ZPole} = 2; N_{Isolep} = 2; l_1 = e, l_2 = \mu$	122	145	150
$N_{Remain} < 3$	121	113	122
10 GeV $< M_{Inv}^{e\mu} <$ 65 GeV	116	101	87
$M_{Missing} < 65$ GeV$/c^2$	110	26	36
$\sqrt{(\frac{D0}{sigD0})^2 + (\frac{Z0}{sigZ0})^2} < 5$	93	3	10

Table 4: The final event selection of $e^+e^- \to ZH, Z \to \mu^+\mu^-, H \to WW^*, WW^* \to e\nu\mu\nu$ decay.

Decay Chain	Final States	Number of Events
$e^+e^- \to ZZ, ZZ \to \tau^+\tau^-\mu^+\mu^-$	$\mu^+, \mu^-, \tau^+, \tau^-$	10

Table 5: Summery of total background with the same final states of signal event

3.1.2 Statistical result

After selection, we can get the distribution of recoil mass of $\mu^+\mu^-$, as shown in Figure 3.1.2.

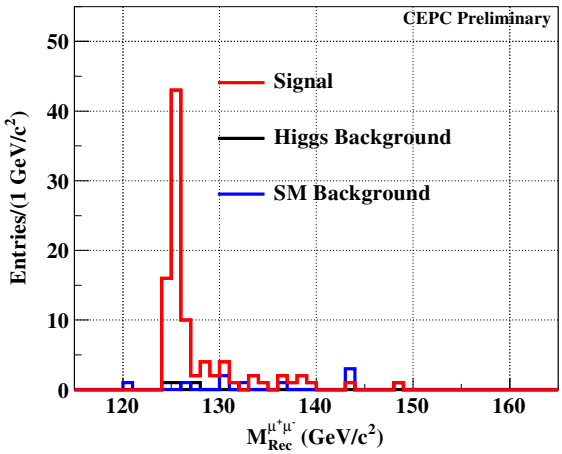

Figure 8: The distribution of recoil mass of $\mu^+\mu^-$ after event selection

Number of signal events could be got by counting,

$$N_{sig} = 93 \pm 10;$$

and N_{sig} is events of signal, the efficiency of selection $\varepsilon = 54.1\%$. Statistical uncertainty is

$$Accu. = \frac{\sqrt{S+B}}{S} = 11\%.$$

3.2 Analysis of $e^+e^- \to ZH, Z \to e^+e^-, H \to WW^*, WW^* \to \mu\nu q\bar{q}$ decay

3.2.1 Event selection

In this decay chain, number of signal events is much larger than the full-leptonic final states although still not as clear as $ev\mu\nu$ channel, so we could get a higher accuracy. The final state consists of three leptons, several jets and neutrinos. The fully leptonic decay background of τ events would be rejected by number of remain particle less than 30 and larger than 7.

As mentioned before, invariant mass and corresponding recoil mass of two leptons from initial Z boson are effective criteria to suppress the Standard Model background. So validation of pre-selection, $80\ \mathrm{GeV}/c^2 < M_{Inv}^{e^+e^-} < 100\ \mathrm{GeV}/c^2$ and $120\ \mathrm{GeV}/c^2 < M_{Rec}^{e^+e^-} < 150\ \mathrm{GeV}/c^2$ are applied.

The jets come from different ways,such as Higgs decay, W boson decay, Z boson decay and τ decay. Based on this, the invariant mass of jets, $10\ \mathrm{GeV}/c^2 < M_{Rec}^{di-Jet} < 95\ \mathrm{GeV}/c^2$, could distinguish the signal and background well. And b-jet would not come from W boson, so we could use b-tagging to vote the b-jet background.

In signal, here is only one isolated muon from W boson and its start point is near the IP, so background of muon from τ or jet could be rejected powerfully by a function. The form of this function is similar with before, $\sqrt{(\frac{D_0}{sigD_0})^2 + (\frac{Z_0}{sigZ_0})^2} < 4$. In order to veto background of t channel, transverse momentum $p_T > 5$ GeV has applied.

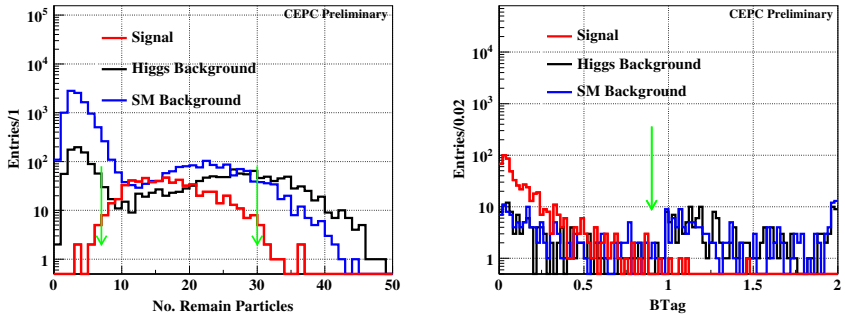

(a)

(b)

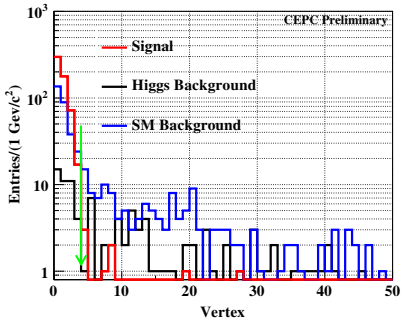

(c)

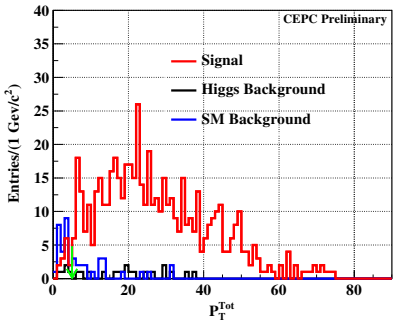

(d)

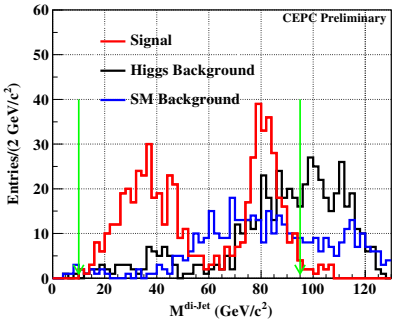

(e)

Figure 9: 9(a) The No. remain particles of $e^+e^- \to ZH, Z \to e^+e^-, H \to WW^*, WW^* \to \mu\nu q\bar{q}$ decay. Because it is semi-leptonic decay channel, so the No. remain particles should between it of hadronic decay and full-leptonic decay. 9(b) The distribution of Btag, we plus the Btag value of each jets because of existing two jets. And because no b-jet decay from W boson, the value of them should be less than 1. 9(c) The distribution of vertex of lepton. Leptons from τ and b-jet would fly a long distance, so they would be rejected effectively. 9(d) The distribution of transverse momentum p_T. Transverse momentum of t channel would be lower than of s channel. 9(e) The distribution of di-jet invariant mass, the high-side could distinguish the jets from Z boson or H boson.

After the selection as shown in Table 6, the background are suppressed almostly. Table 7 shows the main background after event selection.

Category	Signal	ZH background	SM background
Total	1149	36319	1303847
$N_{ZPole} = 2; N_{Isolep} = 1; N_{Jets} = 2; l = \mu$	1022	1970	21857
Validation of pre-selection	631	1207	2987
$7 < N_{Remain} < 30$	603	540	436
$15\ \mathrm{GeV}/c^2 < M_{Rec}^{di-Jet} < 95\ \mathrm{GeV}/c^2$	589	284	278
$Btag < 0.9$	584	116	131
$M_{Missing} < 45\ \mathrm{GeV}/c^2$	571	72	102
$\sqrt{(\frac{D0}{sigD0})^2 + (\frac{Z0}{sigZ0})^2} < 4$	564	23	45
$p_T > 5$ GeV	551	18	21

Table 6: The final event selection of $e^+e^- \to ZH, Z \to e^+e^-, H \to WW^*, WW^* \to \mu\nu q\bar{q}$ decay

Decay Chain	Final States	Number of Events
$e^+e^- \to ZH, Z \to e^+e^-, H \to WW^* \to \tau\nu q\bar{q}$	$e^+, e^-, \tau, \nu, 2q$	14
$e^+e^- \to e^+e^-Z, Z \to qq$	$e^+, e^-, 2q$	13

Table 7: Summery of total background with the same final states of signal event

3.2.2 Statistical result

After selection, the distribution of recoil mass of e^+e^- is shown in Figure 3.3.2.

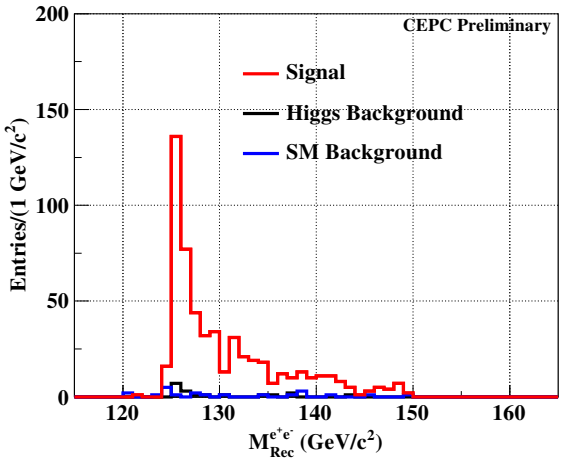

Figure 10: The distribution of recoil mass of $\mu^+\mu^-$ after event selection

We can get the number of signal events by counting,

$$N_{sig} = 551 \pm 24;$$

and N_{sig} is events of signal, the efficiency of selection $\varepsilon = 48.0\%$. Statistical uncertainty is

$$Accu. = \frac{\sqrt{S+B}}{S} = 4.5\%.$$

3.3 Analysis of $e^+e^- \to ZH, Z \to \nu\bar{\nu}, H \to WW^*, WW^* \to q\bar{q}q\bar{q}$ decay

3.3.1 Event selection

This is a hadronic decay channel and no isolated lepton. Lost of the Standard Model background would not be suppressed by no isolated lepton and at least two jets. The number of final particles is required to be larger, $No._{Particles}^{Total} > 20$, because the final particles are produced a lot after hadronization of quarks. And fraction of hadronic process would be enhanced a lot by this requirement.

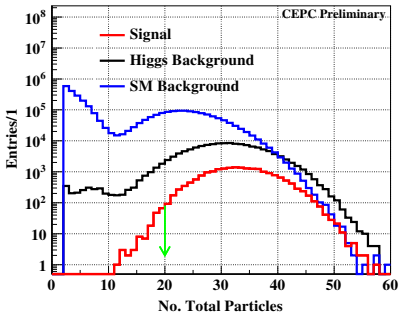

Figure 11: The number of total final particles distribution. To count the total number, the energy threshold of each particle is required, $E > 1$ GeV

The the jet clustering has been done twice. At the first time, two jets are clustered to reject the two jets background, such as $H \to q\bar{q}$ decay of Higgs background, ZZ semi-leptonic decay and "single $Z - nu$" semi-leptonic decay process of the Standard Model background. These two jets are required $Btagging < 0.9$, $Cos\theta_{2jets} > 0.87$ and $\Sigma|M_{Inv}^{2jet}| > 50\ \mathrm{GeV}/c^2$. And at the second time, four jets are required. In this situation, the characterizes of signal are more important. Y value is effective to distinguish the signal and background. The event is required to have $Y_{34} > 0.005$. According to these four jets, we would get two components which are the combination of four momentum of among two jets. The invariant mass of one of the components should be near the mass peak of the W boson, and the jets in the other part are regard as from virtual W boson decay. Figure 13(b) shows the distribution of these two component. The combined functions are:

- $65\ \mathrm{GeV}/c^2 < M_{Inv}^{Real4jet} < 85\ \mathrm{GeV}/c^2$;
- $15\ \mathrm{GeV}/c^2 < M_{Inv}^{Virt4jet} < 50\ \mathrm{GeV}/c^2$;
- $M_{Inv}^{Virt4jet} > -7/3 M_{Inv}^{Real4jet} + \frac{605}{3}\ \mathrm{GeV}/c^2$;

$M_{Inv}^{Real4jet}$ means invariant mass of two jets which are regard as jets decay from real W boson. And $M_{Inv}^{Virt4jet}$ means invariant mass of two jets which are regard as jets decay from virtual W boson.

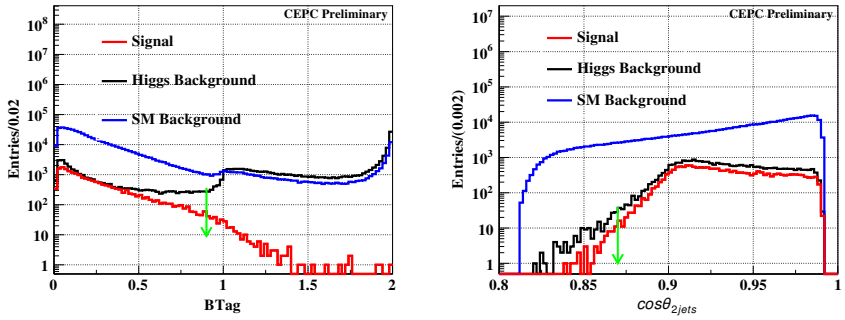

(a)

(b)

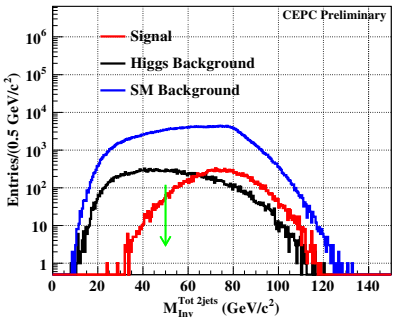

(c)

Figure 12: 12(a) B-tag of two jets distribution. We plus the value of B-tag of each jet, 12(b) The distribution of angle between two jets. The boost of Higgs is larger, so the angle between two jets in signal should be smaller its in background. 12(c) The distribution of total invariant mass of two jets. The number of jets in almost background is two. The invariant mass of each jet should be smaller.

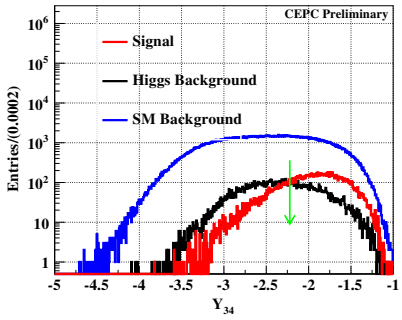

(a)

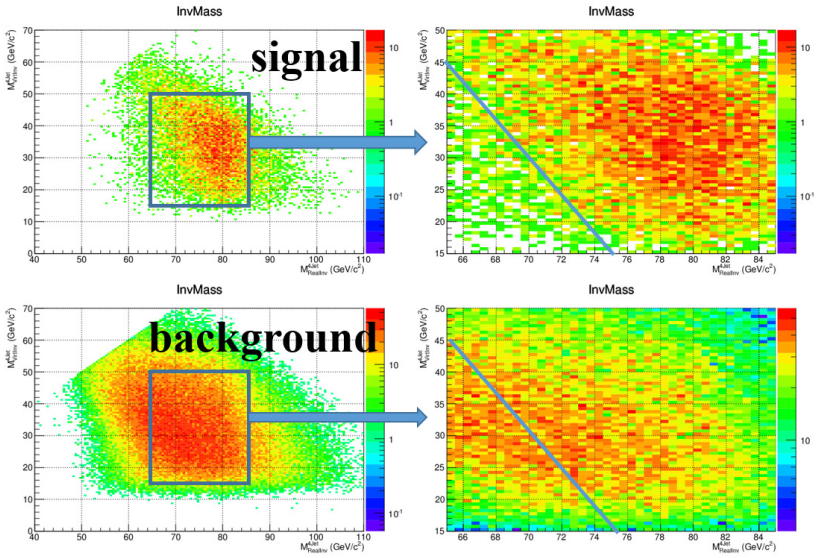

(b)

Figure 13: 13(a) Y value distribution. 13(b) 2D scatter diagram of invariant mass of real and virtual W boson. The left plot represents the distribution of signal, and the right is of background. In order to distinguish the signal and background effectively, a hexagonal mass window is applied.

178 After the event selection, the signal is protected near 50% as shown in Table 8

Category	Signal	ZH background	SM background
Total	23938	208200	21314314
Validation of pre-selection	20405	143765	3166923
$N^{Tot}_{Particle} > 20$	19681	124112	537839
$Btag < 0.9$	19349	28857	477099
$Cos\theta_{2jets} > 0.87$	19298	28673	433563
$\Sigma\lvert M^{2jet}_{Inv}\rvert > 50$ GeV	18621	14793	309919
$Y_{34} > 0.005$	15183	6919	122866
Combined Variable	9022	3075	38226

Table 8: The final event selection of $e^+e^- \to ZH, Z \to \nu\bar{\nu}, H \to WW^*, WW^* \to q\bar{q}q\bar{q}$ decay

Decay Chain	Final States	Number of Events
$e^+e^- \to ZH, Z \to \nu\bar{\nu}, H \to c\bar{c}$	$\nu, \bar{\nu}, c, \bar{c}$	192
$e^+e^- \to ZH, Z \to \nu\bar{\nu}, H \to b\bar{b}$	$\nu, \bar{\nu}, b, \bar{b}$	352
$e^+e^- \to ZH, Z \to \nu\bar{\nu}, H \to gg$	$\nu, \bar{\nu}, 2g$	2028
$e^+e^- \to ZH, Z \to \nu\bar{\nu}, H \to ZZ^*, ZZ^* \to q\bar{q}q\bar{q}$	$\nu, \bar{\nu}, 2q, 2\bar{q}$	439
$e^+e^- \to ZZ, ZZ \to \nu\bar{\nu}q\bar{q}$	$\nu, \bar{\nu}, q, \bar{q}$	3115
$e^+e^- \to ZZ, ZZ \to \tau^+\tau^- q\bar{q}$	$\tau^+, \tau^-, q, \bar{q}$	910
$e^+e^- \to WW, WW \to \tau\nu q\bar{q}$	$\tau, \nu, q, \bar{q}$	30398
$e^+e^- \to WW, WW \to \mu\nu q\bar{q}$	$\mu, \nu, q, \bar{q}$	277
$e^+e^- \to \nu\bar{\nu}Z, Z \to q\bar{q}$	$\nu, \bar{\nu}, q, \bar{q}$	1838
$e^+e^- \to e\nu W, W \to e\nu q\bar{q}$	$e, \nu, q, \bar{q}$	1398
$e^+e^- \to qq$	$2q$	262

Table 9: Summery of main background with the same final states of signal event

3.3.2 Statistical result

After selection, we can get the distribution of missing mass, as shown in Figure **??**.

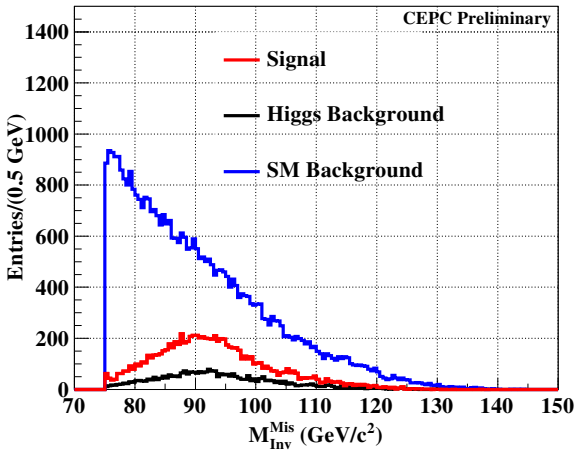

Figure 14: The distribution of recoil mass of $\mu^+\mu^-$ after event selection

We can get the number of signal events by counting,

$$N_{sig} = 9022 \pm 224;$$

and N_{sig} is events of signal, the efficiency of selection $\varepsilon = 37.7\%$. Statistical uncertainty is

$$Accu. = \frac{\sqrt{S+B}}{S} = 2.5\%.$$

4 Results

The function of measurement of branch ratio of $H \to WW^*$ is

$$Br(H \to WW^*) = \frac{N_{sig}}{N_{total} \cdot Br_{rel.} \cdot \varepsilon}$$

$N_{total} = \mathcal{L} \times \sigma_{ZH}$ means total number of events of ZH process; $Br_{rel.}$ means relative branch ratio for $Br(H \to WW^*)$ measurement, including branch fraction of Z boson and W boson; ε means the efficiency of event selection of signal; N_{sig} means the events of signal after event selection.

Category	Signal	Relative uncertainty	Efficiency of selection
$Z \to e^+e^-; H \to WW^* \to evev$	20±7	35%	25.0%
$Z \to e^+e^-; H \to WW^* \to \mu\nu\mu\nu$	44±8	18.2%	43.1%
$Z \to e^+e^-; H \to WW^* \to ev\mu\nu$	53±8	15.1%	27.6%
$Z \to e^+e^-; H \to WW^* \to evqq$	435±23	5.3%	37.0%
$Z \to e^+e^-; H \to WW^* \to \mu\nu qq$	551±24	4.5%	48.0%
$Z \to \mu^+\mu^-; H \to WW^* \to evev$	23±5	21.7%	25.8%
$Z \to \mu^+\mu^-; H \to WW^* \to \mu\nu\mu\nu$	39±7	18%	44.8%
$Z \to \mu^+\mu^-; H \to WW^* \to ev\mu\nu$	93±10	11%	54.1%
$Z \to \mu^+\mu^-; H \to WW^* \to evqq$	573±25	4.0%	51.7%
$Z \to \mu^+\mu^-; H \to WW^* \to \mu\nu qq$	756±30	4.4%	68.4%
$Z \to \nu\bar{\nu}; H \to WW^* \to qqqq$	9022±224	2.5%	37.7%

Table 10: Statistic uncertainty of Signal and Relative uncertainty

	Total events N	$Br(W \to l\nu)$	$W \to qq$	$Z \to l^+l^-$	$Z \to qq$
Mean value	1060000	10.86%	67.41%	3.3658%	69.91%
Uncertainty	±4000	±0.09%	±0.27%	±0.0023%	±0.06%

Table 11: Relative data for measurement of branch ratio

After analysis, the relative uncertainty of signal of 11 decay chains is given in Table 10, and the result of each branch ratio is given by other collaboration in Table 11. The relative uncertainties of $Z \to X$, $W \to X$ and N_{Total} are negligible. Relative statistical uncertainty $\Delta Br(H \to WW^*)/Br(H \to WW^*)$ is 1.62%.

5 Summary and conclusion

In total, eleven different final states originating from $H \to WW^*$ decays have been analyzed at CEPC. The study assumes an integrated luminosity of 5000fb$^-$1 and a SM Higgs boson with mass of 125 GeV. The obtained result indicates that the branching ratio BR($H \to WW^*$) can be measured with an uncertainty of just 1.62%.

Recently, only about 15% data has been analyzed. With the CEPC R&D goes by, the result of analysis would be optimized continuously. In the future, $Z \to qq, H \to WW^* \to qqqq$ channel would be analyszed, which would improve the accuracy effectively for measurement of branch ratio. Furthermore, CEPC is also a Z boson factory, and it would give us a great support. On the one hand, the precision of measurement result about Z boson would be improved, and it would be helpful for precise measurement at CEPC. On the other hand, a huge sample would be produced at Z pole, and it would help us to study the performance of detector better and reduce the systematic uncertainty.

Later on, there are three parts to be considered. At first, systematic uncertainty has not be discussed. And we would do it in the future. Secondly, the isolated lepton finder algorithm is not a general algorithm, and needs to be optimized and improved, but it is suitable for recent research. At last, events of signal

are got by counting, and we should learn the distribution of signal and background deeper and do a fit to improve precision of analysis.

6 Acknowledgements

Thanks Dr. LI Gang and Dr. RUAN Manqi greatly for their guidance and their constructive arguments. And thanks my colleagues, Mr. CHEN Zhenxing and Mr. WEI Yuqian who build a good basement for me, Dr. MA Bingsong and Dr. MO Xin who are engaged in generator, simulation and reconstruction of samples, Dr. WANG Feng who help me solve some technical problems.

References

[1] R. M. CHEN Zhenxing, LIU Shuai,, "Measurement of higgs to ww at cepc." Available from the cepc note web page: Http://cepcdoc.ihep.ac.cn/docdb/0000/000041/001/ww_v1.0.pdf.

Appendices

A Isolated leptons' condition

Isolated leptons tagging is a key in WW^* analysis, especially in jets environment, so a good iaolated leptons algorithm could decide our analysis accuracy. We will introduce the isolated leptons algorithm below:
There are two key conditions. The first one is lepton identification that a good PFA could help us. The second is isolated conditions, cone angle of lepton and the ratio of energy in cone angle and lepton's energy, shown in Table 12.

E_{lepton}	Leptons' flavor	Full-leptonic Decay		Semi-leptonic Decay	
		Cone Angle[rad]	E_{Cone}/E_{Lepton}	Cone Angle[rad]	E_{Cone}/E_{Lepton}
5 GeV – 10 GeV	Muon	0.15	0.25	0.15	0.7
	Electron	0.3	1.1	0.3	0.9
10 GeV – 15 GeV	Muon	0.15	0.35	0.15	0.25
	Electron	0.3	0.75	0.3	0.75
> 15 GeV	Muon	0.15	0.3	0.15	0.25
	Electron	0.25	0.55	0.25	0.6

Table 12: Isolated lepton condition